Bio-Design and Manufacturing (2026) 9:94–99
https://doi.org/10.1631/bdm.2500162

CASE REPORT

AI-assisted design of 3D-printed prosthesis for integrated replacement of the hip, femur, and knee caused by osseous hydatidosis

Yanlong Han[1] · Haoyuan Lei[2] · Ruozhen Jia[1] · Wei Zhao[1] · Habaxi Kaken[1] · Deli Wang[4] · Yongsheng Liu[5] · Zhen Tan[4] · Li Wang[1] · Changchun Zhou[1,2,3]

Received: 2 April 2025 / Accepted: 24 July 2025 / Published online: 27 October 2025
© Zhejiang University Press 2025

Graphical abstract

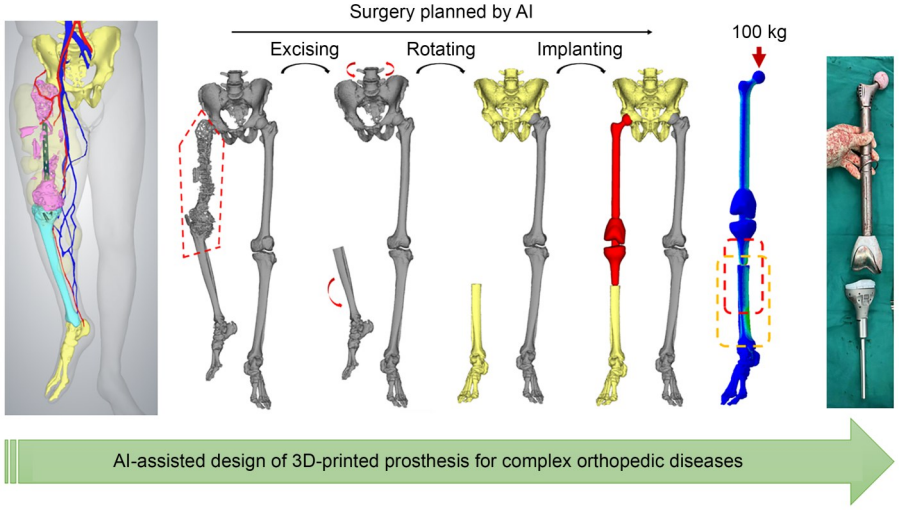

Cases of widespread bone hydatid infection are relatively rare in clinical practice. In this study, we reported for the first time a validated integrated repair therapy for multiple bone tissues, including the hip, femur, and knee, caused by echinococcosis. Artificial intelligence (AI) was used to develop a targeted surgical plan and to design a personalized prosthesis. Finite element analysis (FEA) was used to optimize the mechanical effectiveness of a customized integrated replacement prosthesis and to model stress distribution in the surrounding bone. Three-dimensional (3D) printing was used to fabricate a customized prosthesis. With the assistance of AI, FEA, and 3D printing technology, a personalized surgical plan and customized prosthesis were successfully constructed based on the patient's disease. This approach achieved a

✉ Zhen Tan
tanzeric@bjmu.edu.cn

✉ Li Wang
doctorwanglixj@126.com

1 Department of Joint Surgery and Orthopaedics, People's Hospital of Xinjiang Uygur Autonomous Region, Urumqi 830054, China

2 National Engineering Research Center for Biomaterials, College of Biomedical Engineering, Sichuan University, Chengdu 610064, China

3 Tianfu Jincheng Laboratory, Chengdu 610093, China

4 Department of Bone and Joint Surgery, Peking University Shenzhen Hospital, Shenzhen 518036, China

5 Chengdu Advanced Metal Materials Industry Technology Research Institute Co., Ltd., Chengdu 610300, China

successful therapeutic effect, demonstrating that AI-assisted personalized medicine holds great promise for the future.

1 Introduction

Hydatidosis is a parasitic infection caused by the larval form of *Echinococcus granulosus*. The most frequent sites of infection are the liver and lungs. Bone localization is rare even in endemic areas [1–3]. Bone hydatidosis remains latent for an extended period. The disease is slowly progressive, and its treatment combines chemotherapy and surgery. Complete excision of hydatid lesions tends to result in significant bone defects, and amputation is required for more extensive lesions [4]. Prosthetic implant surgery is an effective treatment for severe, extensive bone defects [5, 6]. Cases of widespread bone hydatid infection are relatively rare clinically. In this report, we describe a patient with hydatidosis with substantial involvement of the hip, femur, and knee.

The rapid development of AI has profoundly impacted clinical biomedicine [7]. To predict orthopedic implant cases, AI uses multiple methods to prevent fractures [8]. To select orthopedic implant materials, a method combining 3D printing and robotic technology has been used to provide large-scale personalized orthopedic implants [9]. To shape orthopedic internal implants, the intervention of AI optimizes the design of internal implants with controlled and complex internal structures and corresponding mechanical properties [10], promoting the construction of personalized custom implants, such as dental implants [11], cranial implants [12], and prostheses for tumor reconstruction [13]. Compared with traditionally designed prostheses, AI-assisted intelligent prostheses can provide personalized assistance to each user based on their unique physical conditions and motor deficits [14, 15]. In this study, we developed a targeted surgical plan and designed a personalized prosthesis using AI.

FEA is a computer simulation of physical forces under actual working conditions, utilizing models and research parameters that help evaluate the mechanical behavior of prostheses constructed using AI. In total knee replacement, problems such as postoperative prosthesis loosening, periprosthesis fractures, and prosthesis wear can be addressed through FEA simulations, and considerations include the prosthetic material and component design and alignment [16, 17]. FEA has also been used to evaluate changes in the physical properties of prostheses by structural optimization design and to verify the mitigation of stress shielding and intraoperative bending of orthopedic bone plates [18]. In this study, FEA was used to optimize the mechanical effectiveness of a customized integrated replacement prosthesis and model stress distribution in the surrounding bone.

2 Methods

2.1 Clinical diagnosis

The patient is a 49-year-old male pastoralist with a history of surgery for a femoral shaft fracture in 2000. The patient suffered from postoperative progressive swelling of the right lower limb, increasing in scope and shortening the right lower limb. It was not actively treated due to economic conditions and other reasons. For the past 23 years, the patient had right limb pain and was unable to walk. Four years ago, the lower leg lesions were excised, and the postoperative pathological examination showed hydatidosis. The patient did not take regular oral anthelmintic albendazole after the operation. Recently, the patient sought treatment at several hospitals. The patient came to our hospital because he did not agree with the recommended amputation.

2.2 AI prosthesis design and surgical planning

Hunyuan, Tencent's general-purpose multimodal large language model, was utilized for personalized prosthesis design and surgical planning using its image-to-3D capability. The following steps were taken to design the prosthesis: (1) Based on the clinical diagnosis, doctors hand-drew a two-dimensional (2D) prosthesis sketch; (2) Hunyuan was used to generate an initial 3D model from the sketch; (3) AI optimized this model for smoother edges and realistic rendering to facilitate 3D printing and surgical planning. The surgical planning was carried out as follows: (1) AI reconstructed a 3D model from computed tomography (CT) data to suggest resection boundaries; (2) Hip and tibia orientations were adjusted to optimal angles; (3) The AI-simulated prosthesis was implanted by matching it to residual bone structures.

2.3 Finite element analysis

The optimized prosthesis underwent FEA. *Magics* software adjusted the prosthesis size and position to match the AI-planned resection surfaces of the pelvis and distal tibia. The models were remeshed in 3-matic (mesh size 1 mm, element type C3D4) with verified quality. In Abaqus, the material properties were assigned using our elastic-plastic constitutive model [19] for bone and Ti6Al4V (Table 1). The prosthesis-bone contact was simplified to "Tie" to reduce computation. Two boundary conditions simulated loading: (1) fixed ankle + 100 kg downward hip load; (2) fixed spine + 100 kg upward foot load. Convergence analysis confirmed the mesh, time increment, and contact stability. The von-Mises stress distribution was evaluated.

2.4 3D printing of the prosthesis

The prosthesis model was sliced using *Magics* software and exported as digital information recognizable by a 3D metal additive manufacturing device (M2 Cusing, Concept Laser, Lichtenfels, Germany). TC4 alloy was used as the raw material, and selective laser melting technology was used to print the prosthesis. The printing process was conducted under the protection of high-purity argon gas with an oxygen content of <0.4%.

3 Results and discussion

3.1 Imaging analysis of the lesion area

Clinical examination revealed right lower limb swelling and 15 cm shortening. Right hip passive movement was painful but unrestricted, but active hip and knee movement was absent. Spinal and neurological exams were normal. Laboratory findings (blood counts, erythrocyte sedimentation rate (ESR), C-reactive protein (CRP)) were unremarkable. A chest/abdomen CT showed no hydatid lesions, and vascular studies (Doppler, CT angiography (CTA)) of both lower limbs were normal. Radiographs demonstrated lytic areas in the right femoral head, acetabulum, femur, and proximal tibiofibular joint, with complete femoral shaft dissolution and displaced hardware. Invasion of the right sacral foramen was noted (Fig. 1a). A hip/thigh/knee CT revealed multiple vesicular cystic lesions (the largest being 10 cm×8 cm×4 cm) involving the right hip, thigh, knee, and leg, invading the sacroiliac joint (Fig. 1b), extending through the greater sciatic notch to involve the piriformis and gluteus minimus. Moreover, 3D-printed models of the lesion area (including the bone, tissue, implants, and vasculature) were created for surgical planning and prosthesis fabrication (Fig. 1c).

3.2 AI for prosthesis design and surgical planning

With the continuous development of machine learning algorithms, hardware, and databases, AI technology has made breakthroughs and provided powerful assistance in clinical medicine. In this study, a 3D model of a prosthesis was constructed with AI technology. Based on the clinical diagnosis, a hand-drawn 2D sketch outlined the femoral and tibial/knee replacement components. Hunyuan software's image-to-3D AI processed this sketch to generate an initial model, which featured sharp edges posing risks of stress concentration and tissue damage [20]. AI optimization then created smoother curvatures, demonstrating biomimetic potential through femur-like contours. Material rendering was used to visualize detailed structural features, informing the manufacturing specifications for 3D printing and postprocessing (Fig. 2a). AI was also utilized to formulate the surgical plan using the 3D models. Based on the patient's CT data, AI suggested lesion resection boundaries (inside the red dashed box), preserving the largest amount of the hip and tibial bones. AI was then used to reposition the 3D models of the hip and tibia to guide prosthesis fitting. Next, the previously optimized prosthesis model was automatically adjusted by AI and combined with the bone model to simulate implantation. The prosthesis replaced the resected tissue, connecting the pelvis (via the upper hip component) to the distal tibia (via the lower knee component) to reconstruct support and restore basic function (Fig. 2b). FEA was subsequently utilized to assess the load stress distribution on the prosthesis and bone to evaluate mechanical effectiveness.

3.3 FEA of bone and prosthesis

FEA simulated mechanical loading on the prosthesis and bone. Under a 100 kg downward hip load, stress was distributed across the prosthesis (0–336.7 MPa) and distal tibia (0–33.34 MPa) without deformation. Both remained below material yield strength (Ti alloy: approximately 1000 MPa; cortical bone: approximately 100 MPa), confirming safety (Fig. 3a). Similarly, a 100 kg upward foot load produced safe stresses on the prosthesis (0–189.2 MPa) and pelvis (0–20.00 MPa) without deformation (Fig. 3b). These results demonstrate that the prosthesis provides effective mechanical support under body-weight-equivalent loads, enabling structural reconstruction and functional replacement while distributing stress. This mitigates fracture or dislocation risks at bone-prosthesis junctions by preventing a concentration of localized stress [21–23]. However, despite stresses being below yield strength, fatigue failure risk remains, suggesting postoperative precautions like avoiding unnecessary weight-bearing activities. FEA thus verified the prosthesis's mechanical viability and informed surgical planning.

3.4 Prosthesis implantation

The patient underwent surgery for a complete hydatid cyst and affected bone removal. Guided by a preoperatively

Table 1 Material properties of bone and Ti6Al4V used for FEA

Material	Density (kg/m^3)	Elastic modulus (Pa)	Poisson's ratio	Plastic strain
Bone	1×10^{-6}	12 000	0.3	/
Ti6Al4V	4.43×10^{-9}	118 000	0.3	$\sigma_y=1155+4000\varepsilon_p$

σ_y: yield stress; ε_p: plastic strain

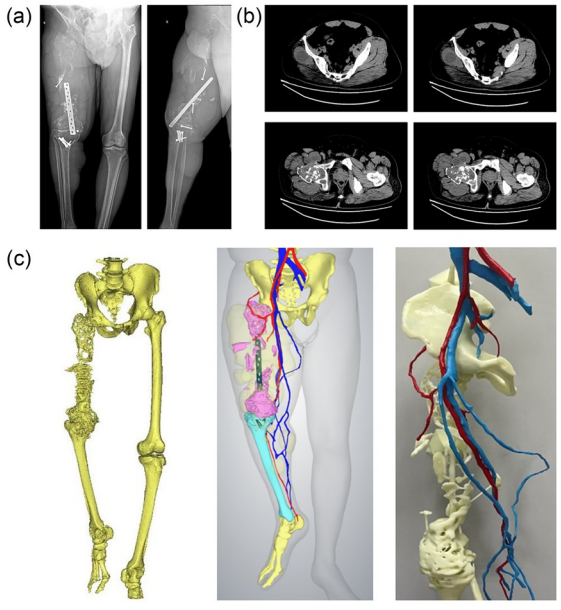

Fig. 1 The reconstruction of lesion area models based on imaging examination. (a) X-ray images showing dispersion of plates and screws and dissolution of the femoral shaft. (b) CT images showing multiple vesicular cystic lesions on the right hip, thigh, knee, and leg. (c) Model reconstruction and 3D printing of the patient's lesion area

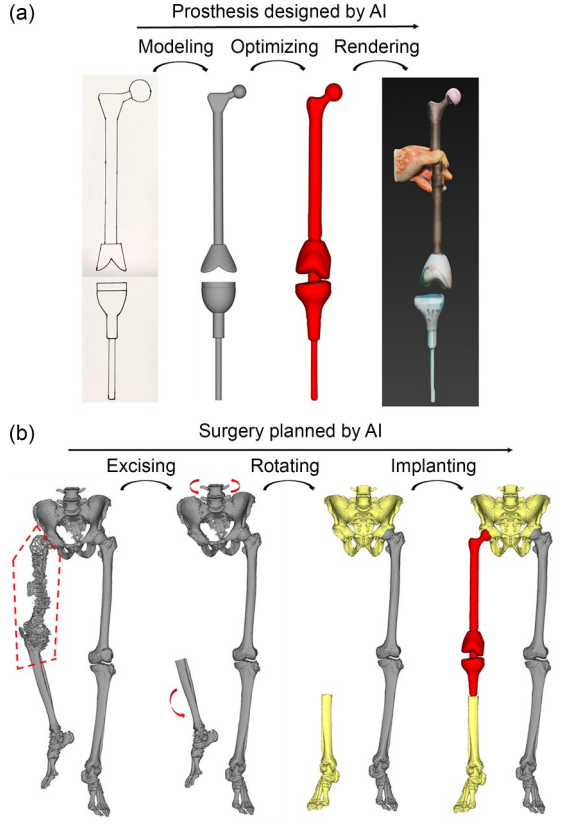

Fig. 2 Using AI for prosthesis design and surgical planning. (a) AI was used to model, optimize, and render the prosthesis from a 2D outline to a 3D structure. (b) AI was utilized for surgical planning in 3D models, encompassing removing diseased bone tissue, rotating the remaining bone, and simulating the prosthetic implantation

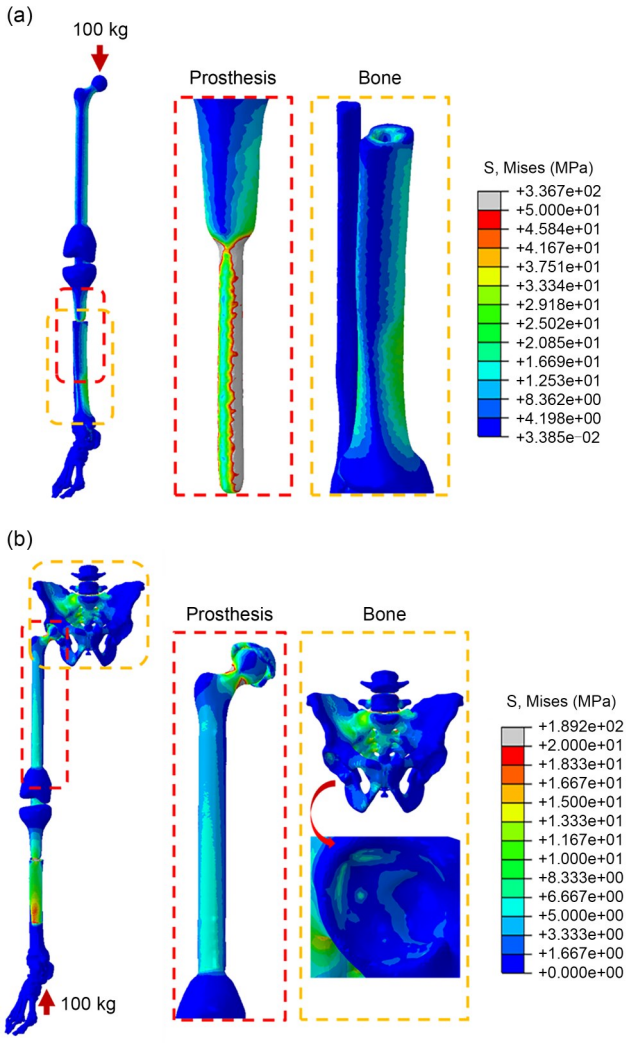

Fig. 3 The equivalent stress distribution under different load conditions. (a) Equivalent stress distribution on the prosthesis and bone surface when a 100 kg load was applied vertically downward from the hip prosthesis. (b) Equivalent stress distribution on the prosthesis and the bone surface when a 100 kg load was applied vertically upward from the bottom of the foot

3D-printed anatomical model and an AI surgical plan, the team precisely resected diseased tissue while preserving healthy structures. The operative field underwent rigorous irrigation with hypertonic saline and iodophor to eradicate residual parasites. AI-designed prostheses were then implanted to reconstruct the hip joint, femoral shaft, and knee articulation. The abductor muscles were sutured to the greater trochanter for prosthesis stabilization (Fig. 4a). Postoperatively, long-term oral albendazole therapy was administered to prevent recurrence. The right lower limb shortening significantly improved (Fig. 4b). Early mobilization involved hip bracing to protect the abductor muscles. By one month postoperatively, the patient achieved full weight-bearing with crutches. At six months, there was no recurrence or discomfort, and the patient reported high satisfaction.

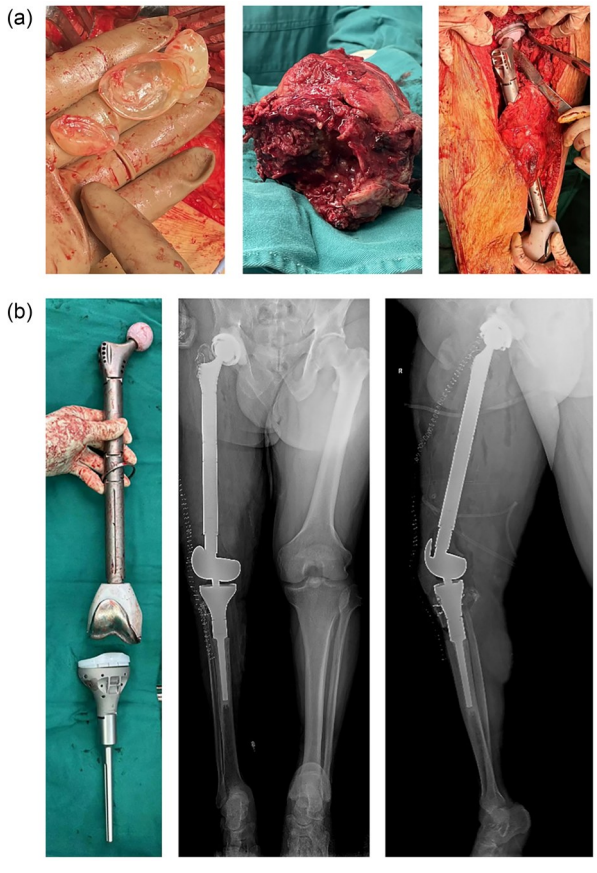

Fig. 4 Intraoperative and postoperative photos and X-rays showed the success of the surgery. (a) Photos of the excision of the hydatid cysts and damaged bone. (b) Photograph and postoperative X-ray images showed good placement of the prosthesis and no recurrence of hydatidosis

4 Conclusions

In summary, this research proposed a combination of AI, reverse engineering, FEA, and 3D printing technologies for precise lesion resection and prosthetic replacement to treat extensive osseous hydatidosis. Considering the complexity of the operation, adequate preoperative preparation and sophisticated planning are essential. AI was utilized to formulate a targeted surgical plan and construct a personalized prosthesis. The mechanical effectiveness of the prosthesis was verified with FEA, which provided a theoretical basis for the structural reconstruction and functional replacement of the customized prosthesis. This approach achieved a successful therapeutic effect, demonstrating that AI-assisted personalized medicine holds great promise for the future.

Acknowledgements This work was partially supported by the National Natural Science Foundation of China (Nos. 32471474 and 82102574), the Precision Medicine Project of People's Hospital of Xinjiang Uygur Autonomous Region (No. 20220305), Chengdu Advanced Metal Materials Industry Technology Research Institute Co., Ltd. Support Project (No. 24H0802), Sichuan Science and Technology Program (Nos. 2025YFHZ0086, 2023YFS0053, 2024YFHZ0125, and 2025ZNSFSC0381), Project of Tianfu Jincheng Laboratory (No. 2025ZH009), Guangdong Basic and Applied Basic Research Foundation (No. 2023A1515220102), and Xinjiang Autonomous Region Science and Technology Support Project Plan (Directive) Project (No. 2024E02049).

Author contributions Writing—original draft: YLH, HYL, RZJ, WZ, HK, DLW, YSL, ZT, LW, and CCZ; writing—review & editing: YLH, HYL, and CCZ; funding acquisition: CCZ and LW; supervision: ZT and LW.

Declarations

Conflict of interest CCZ is an associate editor for *Bio-Design and Manufacturing* and was not involved in the editorial review or the decision to publish this article. The authors declare that they have no conflict of interest.

Ethical approval This study was approved by the Xinjiang Uygur Autonomous Region People's Hospital Ethics Committee (Ethics Number: KY2023031344). Written informed consent (both for participation and publication) was obtained from each patient or the patient's legal guardian.

Data availability The raw data are available from the corresponding authors upon reasonable request.

References

1. Kapoor SK, Kataria H, Patra SR et al (2013) Multi-organ hydatidosis with extensive involvement of the hemi-pelvis and ipsilateral femur. Parasitol Int 62(1):82–85. https://doi.org/10.1016/j.parint.2012.08.006
2. Monge-Maillo B, Tojeiro SC, López-Vélez R (2017) Management of osseous cystic echinococcosis. Expert Rev Anti Infect Ther 15(12):1075–1082. https://doi.org/10.1080/14787210.2017.1401466
3. Muscolo DL, Zaidenberg EE, Farfalli GL et al (2015) Use of massive allografts to manage hydatid bone disease of the femur. Orthopedics 38(10):e943–e946. https://doi.org/10.3928/01477447-20151002-92
4. Zlitni M, Ezzaouia K, Lebib H et al (2001) Hydatid cyst of bone: diagnosis and treatment. World J Surg 25:75–82. https://doi.org/10.1007/s002680020010
5. Zou ZJ, Zou JY, Zhang WG et al (2023) Total femoral replacement for periprosthetic knee joint infection combined with large bone defect: a case report. Asian J Surg 46(12):5792–5794. https://doi.org/10.1016/j.asjsur.2023.08.184
6. Adzhar AL, Faisham WI, Zulmi W et al (2023) Long-term outcome of total femur replacement. Malays Orthop J 17(2):21–27. https://doi.org/10.5704/moj.2307.004
7. Kolomenskaya E, Butova V, Poltavskiy A et al (2023) Application of artificial intelligence at all stages of bone tissue engineering. Biomedicines 12(1):76. https://doi.org/10.3390/biomedicines12010076
8. Leslie WD, Morin SN (2020) New developments in fracture risk assessment for current osteoporosis reports. Curr Osteoporos Rep 18:115–129. https://doi.org/10.1007/s11914-020-00590-7
9. Bandyopadhyay A, Mitra I, Bose S (2020) 3D printing for bone regeneration. Curr Osteoporos Rep 18(5):505–514. https://doi.org/10.1007/s11914-020-00606-2
10. Peltola SM, Melchels FPW, Grijpma DW et al (2008) A review

of rapid prototyping techniques for tissue engineering purposes. Ann Med 40(4):268–280. https://doi.org/10.1080/07853890701881788
11. Roy S, Dey S, Khutia N et al (2018) Design of patient specific dental implant using FE analysis and computational intelligence techniques. Appl Soft Comput 65:272–279. https://doi.org/10.1016/j.asoc.2018.01.025
12. Li JN, Gsaxner C, Pepe A et al (2021) Synthetic skull bone defects for automatic patient-specific craniofacial implant design. Sci Data 8:36. https://doi.org/10.1038/s41597-021-00806-0
13. Tilton M, Lewis GS, Hast MW et al (2021) Additively manufactured patient-specific prosthesis for tumor reconstruction: design, process, and properties. PLoS ONE 16(7):e0253786. https://doi.org/10.1371/journal.pone.0253786
14. Busnatu Ș, Niculescu AG, Bolocan A et al (2022) Clinical applications of artificial intelligence—an updated overview. J Clin Med 11(8):2265. https://doi.org/10.3390/jcm11082265
15. Du X, Chen ZZ, Li QW et al (2023) Organoids revealed: morphological analysis of the profound next generation in-vitro model with artificial intelligence. Bio-Des Manuf 6(3):319–339. https://doi.org/10.1007/s42242-022-00226-y
16. Innocenti B, Pianigiani S, Ramundo G et al (2016) Biomechanical effects of different varus and valgus alignments in medial unicompartmental knee arthroplasty. J Arthroplasty 31(12):2685–2691. https://doi.org/10.1016/j.arth.2016.07.006
17. Park HJ, Bae TS, Kang SB et al (2021) A three-dimensional finite element analysis on the effects of implant materials and designs on periprosthetic tibial bone resorption. PLoS ONE 16(2): e0246866. https://doi.org/10.1371/journal.pone.0246866
18. Vijayavenkataraman S, Gopinath A, Lu WF (2020) A new design of 3D-printed orthopedic bone plates with auxetic structures to mitigate stress shielding and improve intra-operative bending. Bio-Des Manuf 3(2):98–108. https://doi.org/10.1007/s42242-020-00066-8
19. Lei HY, Cao HF, Chen X et al (2025) A functionalized 3D-printed Ti_6Al_4V "cell climbing frame" inspired by marine sponges to recruit and rejuvenate autologous BMSCs in osteoporotic bone repair. Adv Mater 37(11):e2413238. https://doi.org/10.1002/adma.202413238
20. Galteri G, Cristofolini L (2023) In vitro and in silico methods for the biomechanical assessment of osseointegrated transfemoral prostheses: a systematic review. Front Bioeng Biotechnol 11: 1237919. https://doi.org/10.3389/fbioe.2023.1237919
21. Alqazzaz A, Bush AN, Zhuang T et al (2024) Acute total hip arthroplasty following acetabular fracture is associated with a high risk of revision, dislocation, and periprosthetic fracture. J Arthroplasty 39(9S2):S270–S274.e1. https://doi.org/10.1016/j.arth.2024.04.046
22. Wang HW, Wan Y, Li QH et al (2022) Multiscale design and biomechanical evaluation of porous spinal fusion cage to realize specified mechanical properties. Bio-Des Manuf 5(2):277–293. https://doi.org/10.1007/s42242-021-00162-3
23. Zhao DW, Liu BY, Wang F et al (2025) Research and clinical applications of selective laser melting tantalum bone plates. Bio-Des Manuf 8(1):134–149. https://doi.org/10.1631/bdm.2300321